Monthly Notices
of the
ROYAL ASTRONOMICAL SOCIETY

MNRAS **478,** 3825–3831 (2018)
Advance Access publication 2018 May 16

doi:10.1093/mnras/sty1280

New Cepheid variables in the young open clusters Berkeley 51 and Berkeley 55

M. E. Lohr,[1★] I. Negueruela,[2] H. M. Tabernero,[2] J. S. Clark,[1] F. Lewis[3,4] and P. Roche[3]

[1]*School of Physical Sciences, The Open University, Walton Hall, Milton Keynes MK7 6AA, UK*
[2]*Dpto. de Física, Ingeniería de Sistemas y Teoría de la Señal, Escuela Politécnica Superior, Universidad de Alicante, Carretera San Vicente del Raspeig s/n, E-03690 San Vicente del Raspeig, Spain*
[3]*Faulkes Telescope Project, School of Physics and Astronomy, Cardiff University, The Parade, Cardiff CF24 3AA, UK*
[4]*Astrophysics Research Institute, Liverpool John Moores University, 146 Brownlow Hill, Liverpool L3 5RF, UK*

Accepted 2018 May 14. Received 2018 May 11; in original form 2018 April 13

ABSTRACT

As part of a wider investigation of evolved massive stars in Galactic open clusters, we have spectroscopically identified three candidate classical Cepheids in the little-studied clusters Berkeley 51, Berkeley 55, and NGC 6603. Using new multi-epoch photometry, we confirm that Be 51 #162 and Be 55 #107 are bona fide Cepheids, with pulsation periods of 9.83 ± 0.01 d and 5.850 ± 0.005 d respectively, while NGC 6603 star W2249 does not show significant photometric variability. Using the period–luminosity relationship for Cepheid variables, we determine a distance to Be 51 of $5.3^{+1.0}_{-0.8}$ kpc and an age of 44^{+9}_{-8} Myr, placing it in a sparsely attested region of the Perseus arm. For Be 55, we find a distance of 2.2 ± 0.3 kpc and age of 63^{+12}_{-11} Myr, locating the cluster in the Local arm. Taken together with our recent discovery of a long-period Cepheid in the starburst cluster VdBH222, these represent an important increase in the number of young, massive Cepheids known in Galactic open clusters. We also consider new *Gaia* (data release 2) parallaxes and proper motions for members of Be 51 and Be 55; the uncertainties on the parallaxes do not allow us to refine our distance estimates to these clusters, but the well-constrained proper motion measurements furnish further confirmation of cluster membership. However, future final *Gaia* parallaxes for such objects should provide valuable independent distance measurements, improving the calibration of the period–luminosity relationship, with implications for the distance ladder out to cosmological scales.

Key words: stars: variables: Cepheids – open clusters and associations: individual: Berkeley 51 – open clusters and associations: individual: Berkeley 55 – open clusters and associations: individual: NGC 6603 – Galaxy: structure.

1 INTRODUCTION

Evolved stars passing through the instability strip in the Hertzsprung–Russell diagram can exhibit regular pulsations with distinctive light curve shapes and periods, allowing their characterization as – amongst others – δ Scuti, RR Lyrae, or classical/type I Cepheid variables, according to mass (e.g. Chiosi et al. 1992). The detection of Cepheids in Galactic open clusters is valuable in several ways: their presence indicates a relatively young, moderately massive cluster and hence recent star formation activity in the relevant region of the Galaxy; the brevity of the yellow supergiant stage makes such objects intrinsically valuable for constraining models of post-main sequence stellar evolution; the well-known period–luminosity relationship of Cepheids (Leavitt & Pickering 1912) allows their use as standard candles, providing us with a distance tracer for the host cluster and hence enhancing our model of the architecture of the Milky Way; the period–age relationship for Cepheids (Kippenhahn & Smith 1969) can be independently checked through isochrone fitting to the whole cluster population; and finally, future *Gaia* parallaxes for nearby Cepheids can be used to produce an improved calibration of the period–luminosity relationship usable for extragalactic Cepheids, and thus an improved constraint on the Hubble constant (Riess et al. 2018).

Galactic cluster Cepheids are rare: Anderson et al. (2013) identified 23 convincing cases in an eight-dimensional all-sky census, and Chen et al. (2015, 2017) added a further 10, but found that only 31 were usable for constraining the slope of their (near-infrared) period–luminosity relationship. Further valid associations between Cepheids and Galactic open clusters would be of great value.

★ E-mail: marcus.lohr@open.ac.uk

As part of a search for young open clusters containing evolved stars in red and yellow super-/hypergiant stages, where extreme mass-loss rates affect the evolutionary pathways (e.g. Clark et al. 2009; Negueruela et al. 2011; Dorda et al. 2018), we have spectroscopically identified a number of candidate Cepheids, and subsequently undertaken multi-epoch photometry to ascertain their variability status. In Clark et al. (2015) we confirmed the yellow supergiant #505 as a long-period (23.325 d) Cepheid variable in the starburst cluster VdBH222; here, we report our findings on stars #162 and #107, in the faint open clusters Berkeley 51 (Be 51) and Berkeley 55 (Be 55) respectively, in the constellation Cygnus (Negueruela et al. 2018, hereafter N18, and Negueruela & Marco 2012, hereafter N12, respectively). We also report on star W2249 in open cluster NGC 6603, in the constellation Sagittarius. None of these stars were identified as Cepheids or variables of any other type in the second *Gaia* data release.

The three stars are highly probable members of their respective clusters. #162 is in the core of Be 51, as shown in N18 figs 1 and 2, or 34″ from the cluster centre as given on Simbad, where N18 found the cluster to extend to over 3′ from the centre. It lies on the same isochrone as the spectroscopically confirmed B-type cluster members, and the three other F-type supergiants identified in the cluster core (figs 10 and 11 in N18). #107 also lies right in the heart of Be 55 (figs 1 and 2 of N12), at 5″ from the Simbad cluster centre; N12 identified the majority of cluster members as lying within 3′ of the centre, including six of the seven red or yellow supergiants observed. Again, it lies on the same isochrone as B-type confirmed spectroscopic members (figs 9 and 10 in N12). W2249 is 74″ from the centre of NGC 6603; the seven targets – including W2249 – for which radial velocities supported cluster membership (Carrera et al. 2015) lie within 5′ of the centre.

2 DATA ACQUISITION AND REDUCTION

2.1 Spectroscopy

Star #162 in Be 51 was observed in the region of the infrared Ca II triplet on two occasions with the Intermediate dispersion Spectrograph and Imaging System (ISIS) on the 4.2 m William Herschel Telescope (WHT), in 2007 July and 2012 July, as reported in N18. Star #107 in Be 55 was observed on two occasions with ISIS in the same spectral region. The first spectrum, taken in 2007 July, is reported in N12. The second spectrum was taken with exactly the same configuration (unbinned *RED*+ CCD, R600R grating and 1.5 arcsec slit) on 2011 July 26. Finally, a higher resolution spectrum of #107 in the H α region was taken with the Intermediate Dispersion Spectrograph on the 2.5 m Isaac Newton Telescope (INT) on the night of 2017 September 25. The spectrograph was equipped with the *RED*+2 CCD, the R1200R grating and a 1.5 arcsec slit. This configuration provides a resolving power $R \sim 10\,000$ over an unvignetted range of ∼700 Å, which was centred on 6 700 Å.

Parameters for Be 51 #162 were derived in N18 using the STEPAR code (Tabernero et al. 2018); the high-resolution spectrum of Be 55 #107 was used to derive basic stellar parameters by employing the same methodology. As in that case, we fixed the microturbulence ξ according to the 3D model-based calibration described in Dutra-Ferreira et al. (2016), while log g was set to a value of 1.5, typical of similar objects.

For NGC 6603, archival spectra from Carrera et al. (2015) for radial velocity likely cluster members were downloaded and re-reduced to search for evidence of candidate Cepheids.

2.2 Photometry

Time series photometry was obtained for the three clusters using the Las Cumbres Observatory (LCO), described in Brown et al. (2013).[1] For Be 51, 41 usable observations were made between 2015 May 23 and September 19, with both Bessell V and SDSS i' filters (30 s exposures, pixel scale 0.301 arcsec pixel^{-1}). For Be 55, 14 initial observations were made in R between 2017 June 30 and July 29 (10 s exposures, 0.301 arcsec pixel^{-1}); follow-up observations occurred between October 7 and November 5: 18 epochs in R and 15 in V (30 s exposures, 0.387 arcsec pixel^{-1}). For NGC 6603, 20 usable observations were made in R between 2017 July 11 and 30 (10 s exposures, 0.304 arcsec pixel^{-1}).

Basic reductions including bad pixel masking, bias and dark subtraction, and flat-field correction, were performed using the LCO data pipeline. For each cluster, sets of images with a shared pixel scale were rotated if necessary, realigned and trimmed to a common coordinate system and area using the IRAF tasks GEOMAP and IMALIGN. Point spread function (PSF) fitting photometry was then carried out using the IRAF/DAOPHOT package. In each group of images, one frame judged to be of excellent quality – small measured full width at half-maximum (FWHM) of the PSF of isolated bright targets, good signal-to-noise ratio, absence of artefacts – was initially processed to determine the locations of genuine point sources; these coordinates were then used as the starting point for processing all other frames.

After tests with various numbers of PSF stars, functional forms of the analytic component of the PSF model, and orders of empirical variability, the best results were achieved using a three-parameter elliptical Moffat function with $\beta = 2.5$, and an empirical constant PSF model; five PSF stars were selected for each cluster as close to the targets of interest as possible, and covering a comparable range of brightness. Since the observations for each cluster and filter had been made over many nights, under different conditions and often with different instruments, it was necessary to determine the characteristics of each frame individually (FWHM of the PSF of isolated bright stars, sky level, and standard deviation of the sky level) in order to achieve acceptable PSF modelling.

The mid-times of observation of each frame were then converted to BJD(TDB).[2] Using these, light curves could be constructed for all targets believed to be cluster members and bright enough to have magnitudes measured in every frame. Plotting all these together revealed both the typical night-to-night variations associated with changing observing conditions, and the presence of intrinsically variable stars. The light curves of a subset of non-variable objects believed to possess similar spectral types to the candidate Cepheid in each cluster were then combined to produce a reference star, relative to which a differential light curve could be constructed for each suspected variable object. This method resulted in smoother final light curves, with lower uncertainties, than using a single reference star.

3 RESULTS AND DISCUSSION

3.1 Be 51

Spectral variations between the two epochs for suspected Cepheid #162 are evident, despite the different resolutions, as illustrated in

[1]Recent changes to LCO instruments and data products can be found at https://lco.global/observatory/

[2]http://astroutils/astronomy.ohio-state.edu/time/ (see also Eastman et al. 2010)

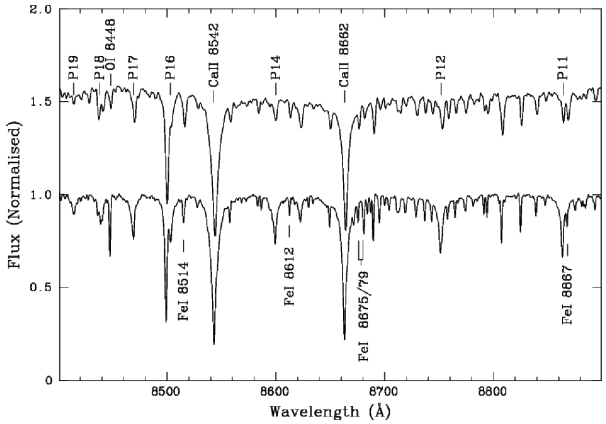

Figure 1. ISIS spectra at two epochs for Be 51 #162 showing changes in spectral type. The upper spectrum is from July 2007, corresponding to an early G type; the lower spectrum, from July 2012 (note the higher resolution), is around F8 Ib. The Paschen and O I 8446 Å lines weaken significantly as we move to G types. Conversely, the general metallic spectrum (some of the strongest Fe I lines are marked) becomes stronger. The apparent inversion of the ratio between the Fe I lines at 8675 and 8679 Å is due to the disappearance of N I 8680 Å, the strongest of a group of N I lines that characterise the spectra of A and F-type stars in this spectral region.

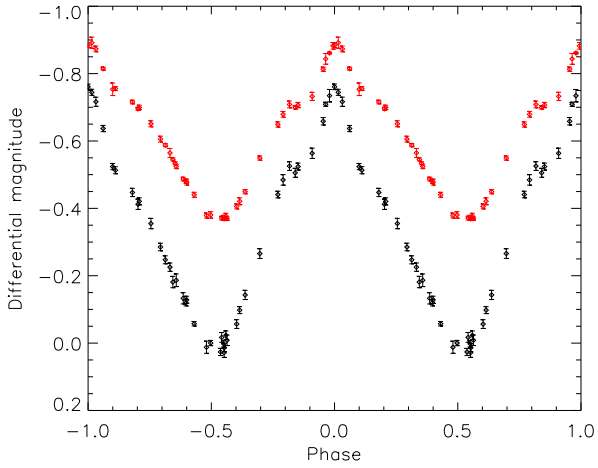

Figure 2. Differential light curves for #162 in V (black, lower curve) and i' (red, upper curve), folded on $P = 9.83$ d, with phase zero set from the V-band maximum. An artificial offset of 0.2 mag between the two curves has been inserted for clarity.

Fig. 1. Parameters for #162 were derived in N18, where it was found to have a very slightly supersolar metallicity.

Initial inspection of the time series photometry for Be 51 revealed clear variability in the light curve of #162, relative to the light curves of other cluster members. No other cluster members studied showed obvious intrinsic variability. A differential light curve was constructed for #162 relative to the combined light curve of four other cluster supergiants (#105, #134, #146, and #172), with mid-F or early K classifications in N18. A period of 9.83 ± 0.01 d was determined for #162 by a form of string length minimization (e.g. Dworetsky 1983), a method well-suited to small quantities of data where the shape of the light curve may not be sinusoidal; however, checks using Lomb–Scargle periodograms (Lomb 1976; Scargle 1982; Horne & Baliunas 1986) and phase dispersion minimization (e.g. Lafler & Kinman 1965; Stellingwerf 1978) confirmed this as the best period in the range 0.5–100 d, and as exceeding the false alarm probability (FAP) 1 per cent threshold. Fig. 2 shows #162's light curves in V and i' folded on this best period. These have the expected shape (according to the Hertzsprung progression, Hertzsprung 1926) of a type I Cepheid of period ∼10 d, with bumps on both ascending and descending branches (compare also fig. 1 in Soszyński et al. 2008). Maxima were obtained at BJD 2 457 202.8815 in V and 2 457 202.8823 in i'.

The V-band photometry for #162 was calibrated using the standardized photometric results from N18, allowing us to determine an average observed magnitude for the Cepheid of $\langle m_V \rangle = 15.295 \pm 0.008$ (range was 14.902 ± 0.006 to 15.688 ± 0.008). An average absolute V-band magnitude was derived from the pulsation period using equation 19 in Anderson et al. (2013): $\langle M_V \rangle = -3.88 \pm 0.24$. An $E(B-V) = 1.79 \pm 0.09$ for #162 was estimated as the mean of the reddenings calculated in N18 for eleven spectroscopically confirmed B-type cluster members [for comparison, $\langle E(B-V) \rangle = 1.76 \pm 0.12$ was estimated for seven supergiants with photometry]; with $R_V = 3.1$, we then obtain $A_V = 5.55 \pm 0.28$. Thus we may calculate a distance to the cluster of $5.3^{+1.0}_{-0.8}$ kpc, where the uncertainties are dominated by the uncertainty in the extinction. Using an alternative calibration of the period–luminosity relationship based on Hubble parallaxes for Galactic Cepheids (Benedict et al. 2007), the distance is $5.7^{+0.8}_{-0.7}$ kpc. Employing the period–age relationship for fundamental mode Cepheids in Bono et al. (2005), an age of 44^{+9}_{-8} Myr is obtained.

These values are consistent with the preferred distance of ∼5.5 kpc found for Be 51 by N18 on the basis of cluster photometry and radial velocities, and with their preferred age for this distance of ∼60 Myr using isochrone fitting to a dereddened colour–magnitude diagram for probable cluster members. In contrast to earlier estimates based on photometry alone, which regarded Be 51 as a much older, closer cluster within the Local arm (Tadross 2008; Subramaniam et al. 2010; Kharchenko et al. 2013), a distance of 5.3 kpc with $\ell = 72\overset{\circ}{.}147$ would seem to place it in the Perseus arm, in a region lacking in reliable distance tracers (see e.g. fig. 11 in Zhang et al. 2013, fig. 14 in Choi et al. 2014, and fig. 5 in Reid et al. 2016).

3.2 Be 55

Again, for Cepheid candidate #107, significant changes in spectral type are seen between the two epochs (see Fig. 3). We also find, for the high-resolution spectrum, $T_{\rm eff} = 5\,505 \pm 199$ K and $[{\rm M/H}] = 0.07 \pm 0.12$, fully consistent with a solar metallicity.

The raw light curves for Be 55 supported significant variability in #107, but also in #198, classified in N12 as a Be shell star (see fig. 8 in N12). Construction of a differential light curve for #198 relative to various subsets of other bright cluster members did not, however, reveal any significant periodicity to this variation, so it may be produced by some aspect of the Be phenomenon (Rivinius et al. 2013) rather than, for example, an eclipsing binary.

The differential light curve for #107 was constructed relative to the combined light curve of four K and G supergiants (#110, #145, #163, and #196 from N12), and its period was determined as 5.850 ± 0.005 d by string length minimization again. This was also confirmed as the most significant periodicity over the range 0.5–100 d by Lomb–Scargle and phase dispersion minimization methods, and far surpassed the 1 per cent FAP threshold. Fig. 4 shows the V- and R-band light curves folded on this period; again, it is apparent that they have the shape of a type I Cepheid with pulsa-

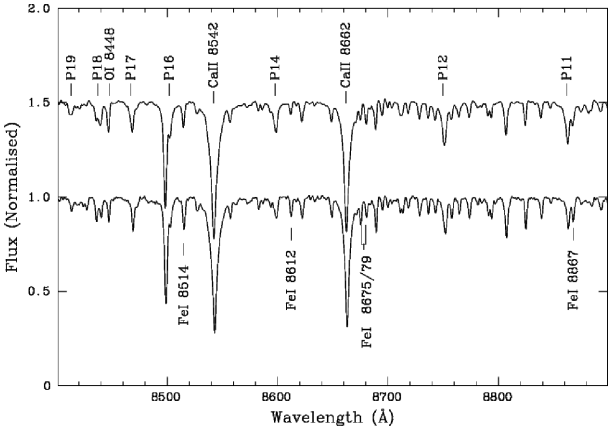

Figure 3. ISIS spectra at two epochs for Be 55 #107 showing changes in spectral type. The upper spectrum, from July 2007, presents a spectral type F8 Ib, while the lower spectrum, taken in July 2011, is early G. Changes are similar to those seen in Be 51 #162 (Fig. 1).

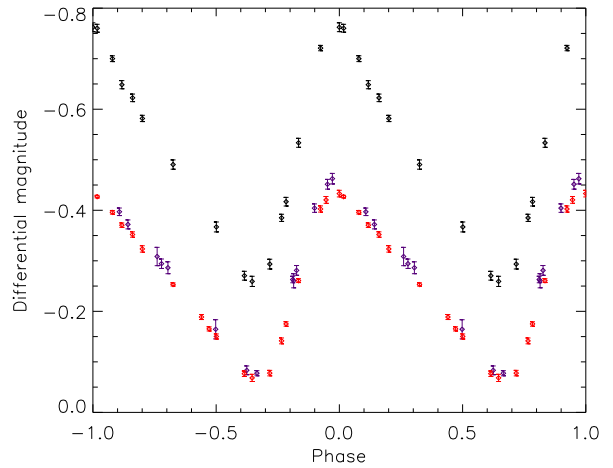

Figure 4. Differential light curves for #107 in V (black, upper curve) and R (purple and red, lower curves), folded on $P = 5.85$ d. The small vertical offset between the two R-band curves and their different uncertainty sizes are caused by the different exposure lengths and pixel scales of the two sets of observations.

tion period ∼5 d, without bumps on either branch, and with a linear descending branch. Maxima were observed at BJD 2 458 053.6674 in V and 2 458 053.6664 in R.

The V-band light curve was calibrated using the photometry of N12, giving $\langle m_V \rangle = 13.834 \pm 0.008$ (range was 13.583 ± 0.006 to 14.085 ± 0.009). Using the same approach as for Be 51, $\langle M_V \rangle$ was determined as -3.23 ± 0.21, and $E(B-V)$ as 1.74 ± 0.07 (the mean of the reddenings calculated in N12 for seven spectroscopically confirmed B-type cluster members excluding the Be shell star #198); this gave $A_V = 5.39 \pm 0.22$. Our calculated distance to the cluster is therefore 2.2 ± 0.3 kpc, or using the relationship of Benedict et al. (2007), $2.4^{+0.3}_{-0.2}$ kpc, with an age of 63^{+12}_{-11} Myr.

This distance is somewhat less than the 4.0 ± 0.6 kpc obtained by N12 by a visual fit to the zero-age main sequence on a dereddened $M_V/B-V_0$ diagram for probable cluster members. However, their age estimate of ∼50 Myr is compatible with ours. Moreover, given the evidence supporting #107's membership of Be 55 given in N12, including the central location of #107 within the cluster, and the presence of five other late-type supergiants in close proximity, we

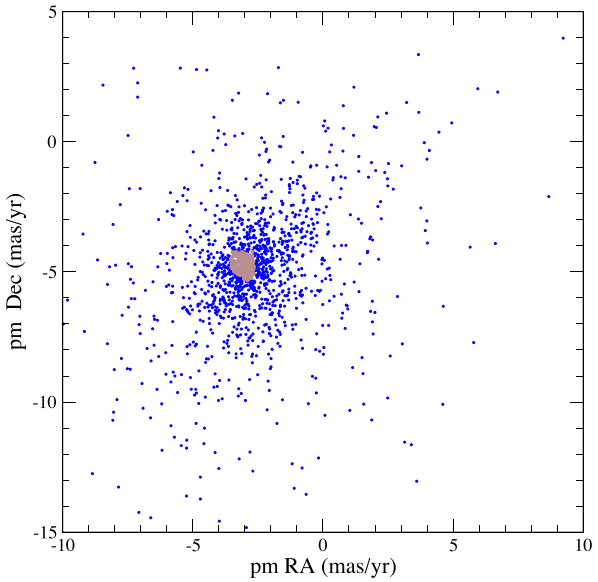

Figure 5. *Gaia* DR2 proper motions for targets within 3′ of the centre of Be 51, showing concentration of selected candidate members in grey.

feel it is more likely that this apparent mismatch is caused by underestimated uncertainties in N12's distance modulus (determined by a single method, rather than the multiple independent approaches discussed in N18), than by an unrelated Cepheid coincidentally lying along our line of sight to the cluster. Earlier purely photometric studies (Maciejewski & Niedzielski 2007; Tadross 2008) had found a even lower distance (1.2 kpc) and much greater age (∼300 Myr), which N12 notes is incompatible with the observed population of B3–4 stars. Our distance of 2.2 kpc with $\ell = 93.^{\circ}027$ would seem to locate Be 55 on the outer edge of the Local arm (Xu et al. 2013, especially fig. 10), rather than in the Perseus arm as N12 suggest.

3.3 NGC 6603

The re-reduced spectrum of object W2249 showed an early G spectral type, similar to the candidate Cepheids in Be 51 and Be 55, motivating further photometric observations. However, no significant variability was detected in its differential light curve, constructed relative to the combined light curves of six other candidate members of NGC 6603 with similar V magnitudes (W1997, W2033, W2215, W2252, W2352, and W2438). The full amplitude of variability exhibited was ∼0.02 mag in R, comparable to the size of the photometric uncertainties.

We may note that age estimates for this cluster are highly inconsistent, ranging from ∼60 Myr (Kharchenko et al. 2005) to ∼500 Myr (Sagar & Griffiths 1998); ages above ∼200 Myr would place it outside a plausible mass range for Cepheids. [This uncertainty in age may be explained by an inappropriate assumption of solar metallicity for the cluster; Carrera et al. (2015) found NGC 6603 to be one of the most metal-rich open clusters known.]

3.4 *Gaia* data release 2

The second *Gaia* data release (*Gaia* Collaboration et al. 2016,2018) made available precise positions, parallaxes, and proper motions for most of the stars previously identified as probable members of Be 51 and Be 55. Therefore we used data release 2 (DR2) data to investigate these clusters afresh. As shown in Figs 5 and 6, the two clusters

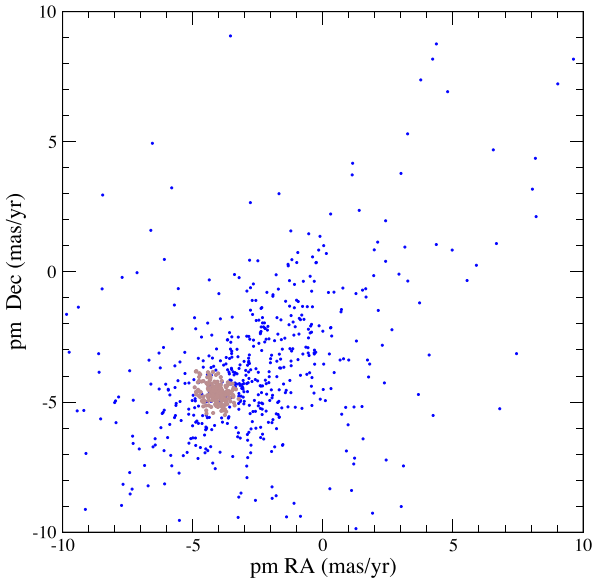

Figure 6. *Gaia* DR2 proper motions for targets within 3.5 arcsec of the centre of Be 55, showing concentration of selected candidate members in grey. This field has a much lower stellar density than that of Be 51, but the cluster members are about two magnitudes brighter, resulting in smaller uncertainties.

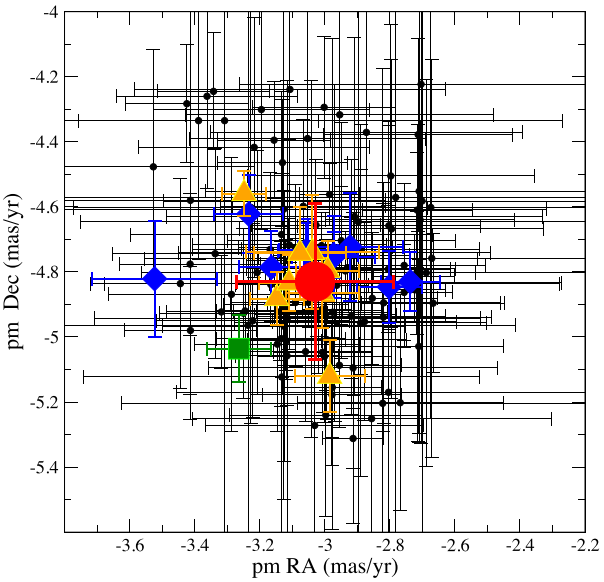

Figure 7. *Gaia* DR2 proper motions, with uncertainties, for cleaned sample of 117 stars identified as probable members of Be 51. The Cepheid #162 is shown with a green square; the eight other cool supergiants (listed in the top panel of N18 table 3) are shown with yellow triangles; B-type stars observed spectroscopically are shown with blue diamonds. One B-type star, #143, is not included here or in Fig. 9 because its astrometric solution in DR2 appears faulty (it has a negative parallax with very large associated uncertainty: -0.36 ± 0.21). The large red circle indicates the weighted average for the cleaned sample, with error bars corresponding to the median uncertainty for single stars: pmRA $= -3.03 \pm 0.20$ mas yr^{-1}, pmDec $= -4.83 \pm 0.24$ mas yr^{-1}.

appear as clear overdensities in the proper motion (pmRA/pmDec) plane, allowing an initial selection of possible cluster members. We then calculated the average proper motion for each cluster, weighting values with the inverse of their uncertainties. Each sample was cleaned iteratively, by discarding outliers and recalculating the average, until the standard deviation of the sample's proper motion was comparable with the median error on an individual value. (Removal of outliers does not imply any judgement on their cluster membership, but simply allows us to define a clean sample of objects with moderately low errors. The procedure is very robust, as the weighted averages do not change significantly throughout.) Figs 7 and 8 show the results for these cleaned samples, with the values for B-type and supergiant stars identified spectroscopically in N12 and N18 highlighted. These reveal that the proper motions fall within a very narrow range for each cluster, and further support cluster membership for almost all of the spectroscopic targets, including, notably, the two Cepheids Be 51 #162 and Be 55 #107.

However, when we investigate parallaxes for these cluster stars, a number of limitations and warnings regarding the DR2 astrometry must be borne in mind, as outlined in Lindegren et al. (2018), Arenou et al. (2018), and Luri et al. (2018). A parallax zero-point of ~ -0.03 mas is found from observations of over half a million quasars (and indeed, comparison with a sample of eclipsing binaries with accurate distances suggests a larger zero-point of -0.08 mas (Stassun & Torres 2018), although the use of a single-star model for all DR2 stars may increase the difference for binary systems). Moreover, there are spatial correlations in parallax and proper motion on scales $\sim 1^\circ$, a number of negative and spurious parallaxes, and parallax uncertainties underestimated by up to 50 per cent for sources in the *G*-band magnitude range 12–15. As a consequence, individual parallaxes for stars beyond 1 kpc are unsafe, and averaging parallaxes over the whole population of an open cluster will not reduce the uncertainty on the mean beyond the ± 0.1 mas level.

With these caveats in mind, we calculated the average parallax for each cleaned cluster sample, again weighting each measurement

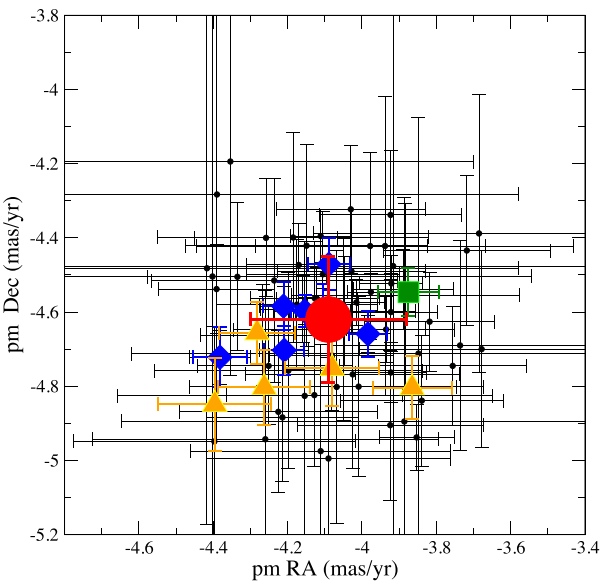

Figure 8. *Gaia* DR2 proper motions, with uncertainties, for cleaned sample of 44 stars identified as probable members of Be 55. The Cepheid #107 is shown with a green square; the five other cool supergiants (listed in N12 table 7, excluding possible foreground interloper S61) are shown with yellow triangles; B-type stars observed spectroscopically are shown with blue diamonds. One B-type star, #129, is not found in DR2. The large red circle indicates the weighted average for the cleaned sample, with error bars corresponding to the median uncertainty for single stars: pmRA $= -4.09 \pm 0.19$ mas yr^{-1}, pmDec $= -4.62 \pm 0.18$ mas yr^{-1}.

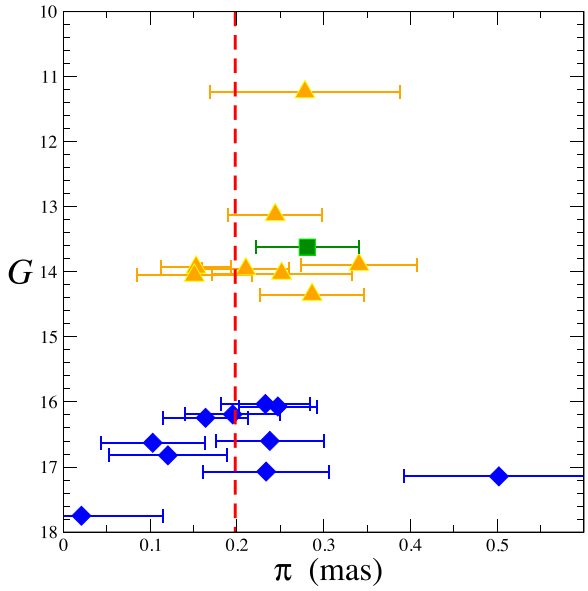

Figure 9. *Gaia* DR2 parallaxes, with uncertainties, against *G*-band mean magnitude for spectroscopically identified B-type and supergiant stars in Be 51 (colours and labels as in Fig. 7). The red dashed line indicates the weighted average parallax for the whole cleaned sample: $\pi = 0.20$ mas, with a standard deviation for the sample of 0.09 mas. The B-type star with the largest parallax is #153, which is also on the edge of the proper motion distribution in Fig. 7; this object could be a non-cluster member, though its astrometric solution may have suffered from the presence of a close companion.

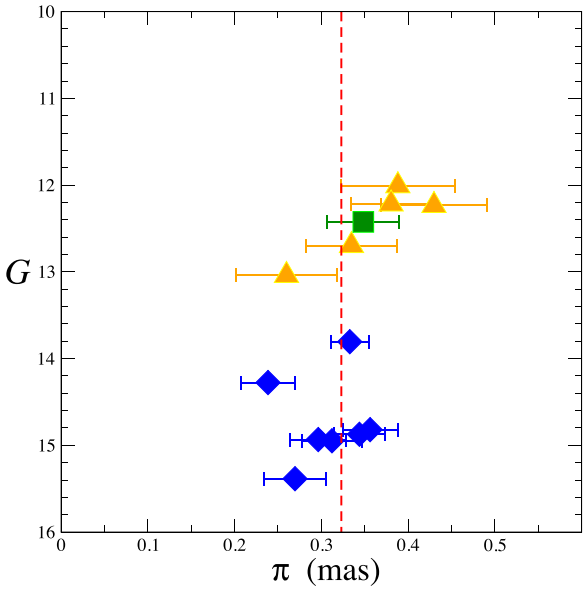

Figure 10. *Gaia* DR2 parallaxes, with uncertainties, against *G*-band mean magnitude for spectroscopically identified B-type and supergiant stars in Be 55 (colours and labels as in Fig. 8). The red dashed line indicates the weighted average parallax for the whole cleaned sample: $\pi = 0.32$ mas, with a standard deviation for the sample of 0.08 mas.

with the inverse of its uncertainty, and removed stars which were incompatible with these average values within their respective uncertainties. (As before, removal of a star does not imply that it is not a cluster member, although many of the removed objects may be expected to be either background or foreground objects unless their errors are very strongly underestimated. Again, the weighted averages are not significantly changed by the cleaning process.) Figs 9 and 10 show the results, plotting only the previously identified supergiants and B-type stars along with the (full) sample average parallaxes. It is notable that the parallaxes of these cluster members are much more widely scattered than their proper motions, and that the supergiants tend to have larger parallaxes than the blue stars, which are concentrated around the cluster averages. Since all objects should be compatible with the average, the uncertainties are clearly underestimated.

Luri et al. (2018) advise against inverting DR2 parallaxes, especially for individual objects, to obtain distances, and instead recommend the use of Bayesian inference for this purpose. However, given the substantial scatter in the parallaxes of Be 51 and Be 55 members, the acknowledged significant underestimation of parallax uncertainties for stars in their magnitude range, and the high and variable extinction in these clusters, we feel such an approach would be of limited value at this stage. So, taken at face value (i.e. using simple inversion of the cleaned cluster sample average parallax), the distance to Be 51 would be ∼5 kpc, with the uncertainties implying a range between 3.3 and 10 kpc. For Be 55, the nominal distance is 3.1 kpc, with an implied range of 2.4–4.5 kpc. Hence, although these distances are consistent with those found earlier in this work and in N12 and N18, we cannot at this stage use *Gaia* DR2 parallaxes to determine distances to Be 51 and Be 55 which are more reliable or precise than those found by other methods.

4 CONCLUSIONS

From spectroscopic and photometric variability, we have confirmed that Be 51 #162 and Be 55 #107 are bona fide classical Cepheids. For #162, we determine a pulsation period of 9.83 ± 0.01 d, implying a distance to Be 51 of $5.3^{+1.0}_{-0.8}$ kpc ($5.7^{+0.8}_{-0.7}$ kpc using another period-luminosity calibration) and an age of 44^{+9}_{-8} Myr, consistent with values found independently in N18, and placing the cluster in a sparsely known region of the Perseus arm. For #107, we find $P = 5.850 \pm 0.005$ d, and hence for Be 55, $d = 2.2 \pm 0.3$ kpc ($2.4^{+0.3}_{-0.2}$ kpc) and age $= 63^{+12}_{-11}$ Myr. This distance would place the cluster in the Local arm. The ages determined for both clusters are also in the interesting range ∼50–60 Myr; as noted in N12, it is rare to find red supergiants in older clusters, so the K supergiants identified in Be 51 and Be 55 may provide valuable data on the boundary between intermediate and massive stars.

Taken together with our Cepheid discovery in Clark et al. (2015), locating the starburst cluster VdBH222 unexpectedly in or near the inner 3 kpc Galactic arm, these new Cepheids in young/intermediate age clusters provide a richer understanding of the architecture of the Milky Way and its recent star formation history. They also represent an important increase in the number of young, massive Cepheids known in Galactic open clusters. While the recent *Gaia* DR2 parallaxes for members of these clusters do not yet allow a reliable check on the distances determined here, future *Gaia* results should provide an independent determination of the distances to such Cepheids and their host clusters, and thereby improve the calibration of the period–luminosity relationship, with implications for the distance ladder out to cosmological scales.

ACKNOWLEDGEMENTS

The Faulkes Telescope Project is an education partner of LCO. The Faulkes Telescopes are maintained and operated by LCO. The WHT and INT are operated on the island of La Palma by the

Isaac Newton Group in the Spanish Observatorio del Roque de los Muchachos of the Instituto de Astrofísica de Canarias. This work has made use of data from the European Space Agency (ESA) mission *Gaia* (https://www.cosmos.esa.int/gaia), processed by the *Gaia* Data Processing and Analysis Consortium (DPAC, https://www.cosmos.esa.int/web/gaia/dpac/consortium). Funding for the DPAC has been provided by national institutions, in particular the institutions participating in the *Gaia* Multilateral Agreement. This work has made use of the WEBDA data base, operated at the Department of Theoretical Physics and Astrophysics of the Masaryk University. This research is partially supported by the Spanish Government Ministerio de Economía y Competitivad (MINECO/FEDER) under grants FJCI-2014-23001 and AYA2015-68012-C2-2-P, and by the UK Science and Technology Facilities Council under grant ST/P000584/1. We thank Dr Carlos González Fernández for obtaining and reducing the 2011 spectrum for Be 55 #107.

REFERENCES

Anderson R. I., Eyer L., Mowlavi N., 2013, MNRAS, 434, 2238
Arenou F. et al., 2018, preprint (arXiv:1804.09375)
Benedict G. F. et al., 2007, AJ, 133, 1810
Bono G., Marconi M., Cassisi S., Caputo F., Gieren W., Pietrzynski G., 2005, ApJ, 621, 966
Brown T. M. et al., 2013, PASP, 125, 1031
Carrera R., Casamiquela L., Ospina N., Balaguer-Núñez L., Jordi C., Monteagudo L., 2015, A&A, 578, A27
Chen X., de Grijs R., Deng L., 2015, MNRAS, 446, 1268
Chen X., de Grijs R., Deng L., 2017, MNRAS, 464, 1119
Chiosi C., Bertelli G., Bressan A., 1992, ARA&A, 30, 235
Choi Y. K., Hachisuka K., Reid M. J., Xu Y., Brunthaler A., Menten K. M., Dame T. M., 2014, ApJ, 790, 99
Clark J. S., Negueruela I., Lohr M. E., Dorda R., González-Fernández C., Lewis F., Roche P., 2015, A&A, 584, L12
Clark J. S. et al., 2009, A&A, 498, 109
Dorda R., Negueruela I., González-Fernández C., 2018, MNRAS, 475, 2003
Dutra-Ferreira L., Pasquini L., Smiljanic R., Porto de Mello G. F., Steffen M., 2016, A&A, 585, A75
Dworetsky M. M., 1983, MNRAS, 203, 917
Eastman J., Siverd R., Gaudi B. S., 2010, PASP, 122, 935
Gaia Collaboration, 2016, A&A, 595:A1
Gaia Collaboration, 2018, preprint (arXiv:1804.09365)
Hertzsprung E., 1926, Bull. Astron. Inst. Netherlands, 3, 115
Horne J. H., Baliunas S. L., 1986, ApJ, 302, 757
Kharchenko N. V., Piskunov A. E., Röser S., Schilbach E., Scholz R.-D., 2005, A&A, 438, 1163
Kharchenko N. V., Piskunov A. E., Schilbach E., Röser S., Scholz R.-D., 2013, A&A, 558, A53
Kippenhahn R., Smith L., 1969, A&A, 1, 142
Lafler J., Kinman T. D., 1965, ApJS, 11, 216
Leavitt H. S., Pickering E. C., 1912, Harv. Coll. Obs. Circ., 173, 1
Lindegren L. et al., 2018, preprint (arXiv:1804.09366)
Lomb N. R., 1976, Ap&SS, 39, 447
Luri X. et al., 2018, preprint (arXiv:1804.09376)
Maciejewski G., Niedzielski A., 2007, A&A, 467, 1065
Negueruela I., Monguió M., Marco A., Tabernero H. M., González-Fernández C., Dorda R., 2018, MNRAS, 477, 2976
Negueruela I., González-Fernández C., Marco A., Clark J. S., 2011, A&A, 528, A59
Negueruela I., Marco A., 2012, AJ, 143, 46
Reid M. J., Dame T. M., Menten K. M., Brunthaler A., 2016, ApJ, 823, 77
Riess A. G. et al., 2018, ApJ, 855, 136,
Rivinius T., Carciofi A. C., Martayan C., 2013, A&AR, 21, 69
Sagar R., Griffiths W. K., 1998, MNRAS, 299, 1
Scargle J. D., 1982, ApJ, 263, 835
Soszyński I. et al., 2008, Acta Astron., 58, 163
Stassun K. G., Torres G., 2018, preprint (arXiv:1805.03526)
Stellingwerf R. F., 1978, ApJ, 224, 953
Subramaniam A., Carraro G., Janes K. A., 2010, MNRAS, 404, 1385
Tabernero H. M., Dorda R., Negueruela I., González-Fernández C., 2018, MNRAS, 476, 3106
Tadross A. L., 2008, MNRAS, 389, 285
Xu Y. et al., 2013, ApJ, 769, 15
Zhang B., Reid M. J., Menten K. M., Zheng X. W., Brunthaler A., Dame T. M., Xu Y., 2013, ApJ, 775, 79

This paper has been typeset from a TEX/LATEX file prepared by the author.